CNS Podcasts Journal Club

Tractography-Based Surgical Targeting for Thalamic Deep Brain Stimulation: A Comparison of Probabilistic vs Deterministic Fiber Tracking of the Dentato-Rubro-Thalamic Tract

Andrew I. Yang, MD, MS[*‡]
Drew Parker, BSc[*§]
Anupa A. Vijayakumari, PhD[§]
Ashwin G. Ramayya, MD, PhD[‡]
Melanie P. Donley-Fletcher, PhD[‖]
Darien Aunapu, BS[§]
Ronald L. Wolf, MD, PhD[¶]
Gordon H. Baltuch, MD, PhD[‡]
Ragini Verma, PhD[‡§¶]

[‡]Department of Neurosurgery, Perelman School of Medicine, University of Pennsylvania, Philadelphia, Pennsylvania, USA; [§]DiCIPHR (Diffusion and Connectomics in Precision Healthcare Research) Lab, Department of Radiology, Perelman School of Medicine, University of Pennsylvania, Philadelphia, Pennsylvania, USA; [‖]Specialty Care Inc, Brentwood, Tennessee, USA; [¶]Department of Radiology, Perelman School of Medicine, University of Pennsylvania, Philadelphia, Pennsylvania, USA

This article was posted to bioRxiv on April 30, 2021, under the title "Tractography-based targeting of ventral intermediate nucleus: A comparison between conventional stereotactic targeting and diffusion tensor imaging-based targeting" (https://doi.org/10.1101/2021.04.29.441001).

*Andrew I. Yang and Drew Parker contributed equally to this work.

Correspondence:
Ragini Verma, PhD,
DiCIPHR (Diffusion and Connectomics in Precision Healthcare Research) Lab,
Department of Radiology,
Perelman School of Medicine,
University of Pennsylvania,
Richards Building, Suite 701A, 3700 Hamilton Walk,
Philadelphia, PA 19104, USA.
Email: Ragini@pennmedicine.upenn.edu

Gordon H. Baltuch, MD, PhD,
Center for Functional and Restorative Neurosurgery,
Penn Neurosurgery,
Pennsylvania Hospital,
Department of Neurosurgery,
Perelman School of Medicine,
University of Pennsylvania,
801 Spruce St,
Philadelphia, PA 19107, USA.
Email: Gordon.Baltuch@pennmedicine.upenn.edu

Received, May 5, 2021.
Accepted, October 25, 2021.
Published Online, January 19, 2022.

BACKGROUND: The ventral intermediate (VIM) thalamic nucleus is the main target for the surgical treatment of refractory tremor. Initial targeting traditionally relies on atlas-based stereotactic targeting formulas, which only minimally account for individual anatomy. Alternative approaches have been proposed, including direct targeting of the dentato-rubro-thalamic tract (DRTT), which, in clinical settings, is generally reconstructed with deterministic tracking. Whether more advanced probabilistic techniques are feasible on clinical-grade magnetic resonance acquisitions and lead to enhanced reconstructions is poorly understood.
OBJECTIVE: To compare DRTT reconstructed with deterministic vs probabilistic tracking.
METHODS: This is a retrospective study of 19 patients with essential tremor who underwent deep brain stimulation (DBS) with intraoperative neurophysiology and stimulation testing. We assessed the proximity of the DRTT to the DBS lead and to the active contact chosen based on clinical response.
RESULTS: In the commissural plane, the deterministic DRTT was anterior ($P < 10^{-4}$) and lateral ($P < 10^{-4}$) to the DBS lead. By contrast, although the probabilistic DRTT was also anterior to the lead ($P < 10^{-4}$), there was no difference in the mediolateral dimension ($P = .5$). Moreover, the 3-dimensional Euclidean distance from the active contact to the probabilistic DRTT was smaller vs the distance to the deterministic DRTT (3.32 ± 1.70 mm vs 5.01 ± 2.12 mm; $P < 10^{-4}$).
CONCLUSION: DRTT reconstructed with probabilistic fiber tracking was superior in spatial proximity to the physiology-guided DBS lead and to the empirically chosen active contact. These data inform strategies for surgical targeting of the VIM.

KEY WORDS: Deep brain stimulation, Dentato-rubro-thalamic tract, Deterministic tractography, Diffusion tensor imaging tractography, Magnetic resonance imaging–guided focused ultrasound, Probabilistic tractography, Ventral intermediate nucleus

Neurosurgery 90:419–425, 2022 DOI:10.1227/NEU.0000000000001840 neurosurgery-online.com

ABBREVIATIONS: ANT, advanced normalization tools; **AP,** anteroposterior; **CC,** craniocaudal; **CRST,** Clinical Rating Scale for Tremor; **CST,** corticospinal tract; **detDRTT,** deterministic dentato-rubro-thalamic tract; **DN,** dentate nucleus; **DRTT,** dentato-rubro-thalamic tract; **ET,** essential tremor; **MER,** microelectrode recordings; **ML,** mediolateral; **MLm,** medial lemniscus; **MRgFUS,** magnetic resonance–guided focused ultrasound; **probDRTT,** probabilistic tractography deterministic dentato-rubro-thalamic tract; **PSA,** posterior subthalamic area; **RN,** red nucleus; **VIM,** ventral intermediate.

Supplemental digital content is available for this article at neurosurgery-online.com.

CNS Journal Club Podcast and CME Exams available at cns.org/podcasts by scanning this QR code using your mobile device.

For the surgical treatment of medically refractory tremor (in the setting of essential tremor [ET] or tremor-dominant Parkinson disease),[1] the target is the ventral intermediate (VIM) thalamic nucleus, which relays signals between the motor cortex and the cerebellum mediating motor control. The VIM is a relatively small anatomic structure (4 × 4 × 6 mm^3; anteroposterior [AP] × mediolateral [ML] × craniocaudal [CC]),[2] which cannot be readily visualized on structural magnetic resonance imaging (MRI) obtained at field strengths typically available in the clinical setting.[3,4] Therefore, the VIM has traditionally been targeted "indirectly" using atlas-based stereotactic targeting formulas that reference neighboring anatomic structures (eg, commissural line and third ventricle).[5] As indirect targeting

provides only an approximation of the location of the VIM, the final surgical target can be further refined with intraoperative microelectrode recordings (MERs) and neurological evaluations concurrent with stimulation.

The goal of this study was to provide an alternative tractography-based localization method for the VIM, which may be particularly useful for interventions in which intraoperative recordings or stimulation testing are not available (eg, magnetic resonance [MR]–guided focused ultrasound [MRgFUS] or "asleep" deep brain stimulation [DBS]). Specifically, there has been much interest in the dentato-rubro-thalamic tract (DRTT), reconstructed using diffusion tensor imaging (DTI) tractography, as an anatomic biomarker of the VIM. Although indirect targeting incorporates patient-specific anatomic parameters (eg, third ventricular width and anterior commissure [AC]–posterior commissure [PC] length), the ability to visualize and target the DRTT from individual patient's MRI provides an opportunity to directly account for intersubject anatomic variability.

According to the classical definition, the DRTT has a decussating pathway (d-DRTT), which emanates from the dentate nucleus (DN), passes through the superior cerebellar peduncle to the contralateral red nucleus (RN)/posterior subthalamic area (PSA), and terminates in the VIM, where it synapses with neurons ascending to the motor cortex (primary motor cortex [M1], premotor cortex, and supplementary motor cortex). These anatomic pathways were first defined in nonhuman primates[6,7] and later in humans on postmortem microdissection and tractography studies.[2,8-10] In addition to the d-DRTT, a nondecussating pathway of the DRTT (nd-DRTT) projecting to the ipsilateral RN/PSA and VIM has also been reported in humans.[11]

There is a multiplicity of published algorithms for DRTT tractography that vary in 2 key aspects. First, different user-defined parameters have been used, particularly for the regions of interest (ROIs) used as seed regions for tractography. These ROIs generally represent a subset of the key structures along the path of the DRTT (as discussed above).[12] Alternatively, Sammartino et al[13] defined a ROI in relation to the neighboring corticospinal tract (CST) and medial lemniscus (MLm). Second, most clinical studies examining DRTT for VIM targeting have applied deterministic fiber-tracking algorithms because of its tractable computational load and integration on commercially available surgical targeting platform. However, deterministic techniques are insensitive to crossing fibers within individual voxels and fail to consistently reconstruct the decussating fibers of the DRTT,[13,14] hindering interpretation of findings when the location of the DRTT is not congruent with the putative location of the VIM localized in the context of DBS or MRgFUS.[15,16] By contrast, probabilistic tracking algorithms are based on higher-order diffusion models, providing better resolution of complex fiber arrangements.

Accurate localization of the VIM is crucial to achieve optimal clinical outcomes in tremor surgery. However, there is a dearth of research comparing the DRTT reconstructed with deterministic vs probabilistic tracking and so whether probabilistic tracking of the DRTT is of any additional clinical value in the context of tremor surgery is poorly understood. In this study, we propose a new protocol for reconstruction of the DRTT with probabilistic tractography (probDRTT). The results were compared with tracts obtained with a widely used deterministic method (detDRTT)[13,17-19] using the location of DBS leads implanted with intraoperative MER and stimulation testing and the empirically chosen active contacts as comparison references.

METHODS

Patient Cohort

We studied 19 patients who underwent DBS surgery for ET (August 2018-February 2019). This cohort was derived from 26 consecutive patients, after exclusion of 7 patients because of unavailability of imaging data (N = 1), poor imaging quality precluding preprocessing (N = 4), or use of different DTI scanning parameters (N = 2). Thirteen patients underwent bilateral implants, and 6 patients underwent unilateral implants (R hemisphere in 2), allowing investigation of 32 DBS leads. Surgical procedure has been previously described in detail.[20] In brief, patients underwent stereotactic placement of DBS leads with the Leksell frame (Elekta, Stockholm, Sweden). MERs were initially obtained along a single tract (center). If units with hand and/or distal upper extremity kinesthetic receptive fields were not identified, additional tracts were sequentially studied. In the current cohort, additional tracts were studied in 3 hemispheres (posterior tract in 2 hemispheres and medial tract in 1). After macrostimulation testing to confirm a satisfactory therapeutic range of stimulation voltages, the DBS lead was implanted such that the most distal contact was at the most distal level at which kinesthetic units were recorded. We note that this study is an extension of previous work that focused on deterministic DRTT.[19] The study protocol was approved by our local Institutional Review Board. All patients provided written informed consent before treatment and imaging acquisition. The Strengthening the Reporting of Observational Studies in Epidemiology (STROBE) guidelines were used in reporting our findings.

MR Acquisitions

Preoperative MRI was acquired at 3T using a 19-channel head coil (Discovery MR750w, GE Healthcare). Imaging data for tractography were acquired with DTI (b-value = 0 s/mm^2, 33 gradient directions with b-value = 2000 s/mm^2, repetition time [TR]/echo time [TE] = 14/0.113, field of view 26 cm, slice thickness = 3 mm, 128 × 128 acquisition matrix, in-plane resolution 1 × 1 mm). Postoperative MRI was acquired at 1.5 T using a 12-channel coil (Optima 450w, GE Healthcare). Locations of the lead/active contact were obtained from T1-weighted spoiled gradient recalled echo (TR/TE = 6.3/1.46 ms, flip angle = 20°, slice thickness = 2 mm, 320 × 256 acquisition matrix, in-plane resolution of 0.43 × 0.43 mm).

Fiber-Tracking Technique

DetDRTT was obtained following published methodology,[13] implemented on DynaSuite Neuro (InVivo Corp, Pewaukee). In brief, a seed region for the DRTT was defined in the bicommissural plane for the CST and MLm, whereby a circular ROI (3-mm radius) was placed such that its center was equidistant from the borders of the CST and MLm.

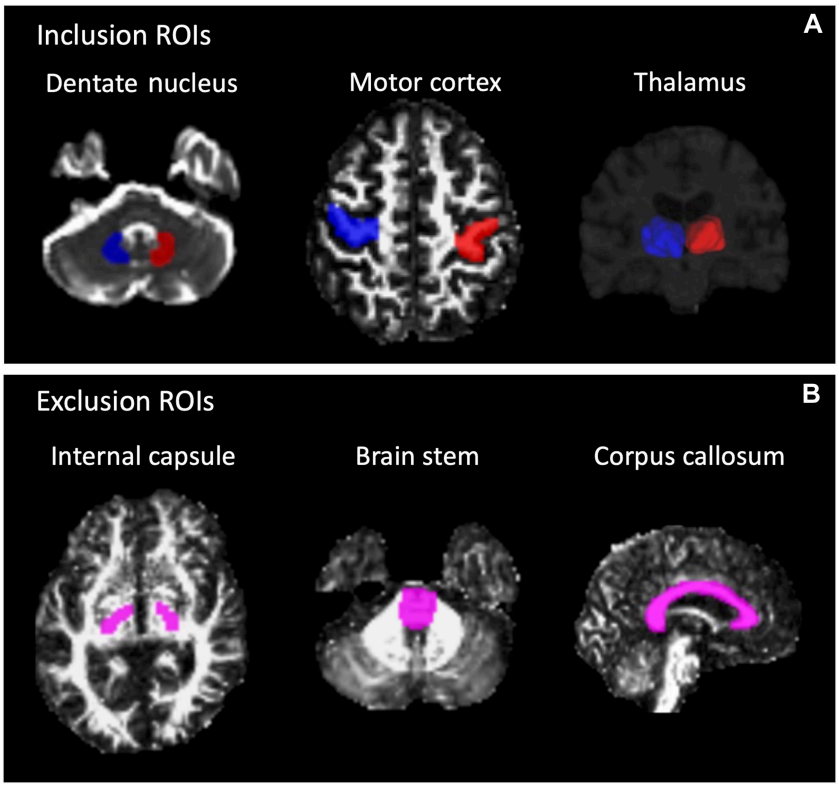

FIGURE 1. *ROIs for probabilistic tractography of the DRTT.* **A**, *Seed ROI (thalamus) and target ROIs (dentate nucleus and primary motor cortex).* **B**, *Exclusion ROIs (internal capsule in the bicommissural plane, ventral brainstem, and corpus callosum). Blue indicates ROIs in the right hemisphere; red indicates ROIs in the left; pink indicates exclusion ROIs. DRTT, dentato-rubro-thalamic tract; ROIs, regions of interest.*

For probDRTT, DTI data sets were denoised (principal components analysis[21]) and corrected for eddy currents and motion artifacts with the eddy[22] tool in the Functional Magnetic Resonance Imaging of the Brain software library.[23] The T1-weighted structural images were bias corrected using the N4 bias correction tool in advanced normalization tools (ANTs),[24] and skull stripping was achieved using the multiatlas region segmentation utilizing ensembles of registration algorithms and parameters[25] (MUSE) methodology. T1 images were coregistered with DTI images using a 6-DOF rigid transformation on ANT. This was followed by a nonlinear registration of the DTI images to the coregistered T1 images using the symmetric image normalization method on ANT which was constrained to the AP direction to correct echo planar imaging distortions.

Constrained spherical deconvolution was performed to estimate the fiber orientation distribution in each voxel using the MRtrix3[26] package. Probabilistic tractography was then performed using the second-order integration over fiber orientation distributions (iFOD2) algorithm.[27] The seed region was the thalamus, which was automatically segmented using FreeSurfer[28] in the T1 images (Figure 1A). The target regions were the hand area of M1 and bilateral DN, which were manually delineated on the fractional anisotropy and B0 images, respectively. Exclusion ROIs were also manually defined to prevent merging with the CST or MLm and consisted of the internal capsule in the bicommissural plane, the corpus callosum, and the ventral portion of the brainstem (Figure 1B). Seeds were then placed randomly across voxels of the thalamus (N = 500), and only streamlines connecting the hand area and bilateral DNs were retained. Tracking was performed with the following parameters: minimum fiber length = 20 mm, maximum fiber length = 250 mm, step size = 0.5 mm, and angle threshold = 45°. Figure 2 shows the probDRTT in an example patient.

Clinical Assessments

DBS programming was conducted empirically based on the patient's clinical response (both tremor reduction and adverse stimulation effects) by neurologists with subspecialty expertise in movement disorders. The cathode was treated as the active contact for monopolar and bipolar stimulation configurations. For interleaved or multipolar configurations, the point in between the 2 cathodes was treated as the active contact. Tremor measurements using the Clinical Rating Scale for Tremor[29] (CRST) questionnaire (treated hand score; range 0-32 points for dominant hand and 28 for nondominant hand, with higher scores indicating greater disability) from before and after DBS were available in a subset of patients (N = 12).

Calculation of Centroids of Implants and Tracts

T1 images were manually AC-PC aligned using ITK-Snap.[30] The track-density images of the DRTT were then registered to the AC-PC–aligned T1 images using the inverse of the rigid transformation described

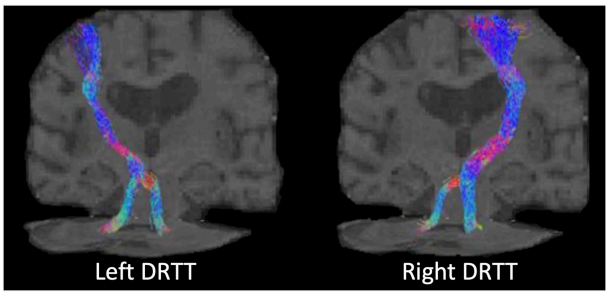

FIGURE 2. *Example DRTT reconstructed in an individual patient. DRTT, dentato-rubro-thalamic tract.*

above.[31] At each axial slice, the centroids of the DRTT were obtained by computing the center of gravity, using the number of fibers from the trace density images (TDI) as weights for each voxel (fslstats tool in FMRIB Software Library). The centroids of the DBS lead in the bicommissural plane and at the level of active contact were also computed (see Methods and Table, **Supplemental Digital Content**, http://links.lww.com/NEU/B50, for details on how the axial slice of the active contact was determined). In the bicommissural plane, the coordinates of the tracts and DBS leads were compared separately in the AP or ML dimension. The 3-dimensional Euclidean distances between the active contact and the tract centroids were calculated at each axial slice. To compare proximity of active contacts to the detDRTT tract vs the probDRTT tract, we used the minimum of these Euclidean distances. A P value of 0.05 was considered statistically significant. All statistical analysis was performed with SPSS (IBM, Armonk).

RESULTS

A total of 19 patients with ET who underwent thalamic DBS (32 leads) were included in this study (Table 1). After implant (3.1 ± 2.4 [mean ± standard deviation] months), treated hand scores of the CRST improved by 66% (paired sample t-test, $P < 10^{-5}$). None of the treated hands had worse tremor postoperatively. In the remaining 7 patients (11 leads) in whom CRST data were not available, none of the patients were noted to be nonresponders on clinical examination.

Of the total 32 implanted hemispheres, probabilistic tractography successfully reconstructed the nd-DRTT and d-DRTT in all hemispheres. By contrast, although the nd-DRTT was visualized in all hemispheres with deterministic tractography, the d-DRTT was reconstructed only in 11 of the 32 hemispheres (31%).

In the bicommissural plane, leads were located 12.05 ± 1.35 mm lateral to the midline and 5.19 ± 0.91 mm anterior to PC (Table 2, Figure 3). The probDRTT was located at 11.76 ± 2.04 mm and 6.64 ± 1.64 mm, respectively. Although the probDRTT was anterior to the lead by 1.45 ± 1.61 mm (paired sample t-test, $P < 10^{-4}$), there was no difference in the ML coordinates (−0.29 ± 2.42 mm; $P = .5$). The detDRTT was located at 14.22 ± 2.27 mm and 6.85 ± 2.21 mm, respectively, which was both lateral (2.16 ± 1.94 mm; $P < 10^{-4}$) and anterior (1.66 ± 2.1 mm; $P < 10^{-4}$) to the lead.

TABLE 1. Demographic and Clinical Characteristics

	Characteristics
No. of DBS patients	19
Age (mean ± SD)	66.05 ± 12.07
Sex (M:F)	10:9
DBS implants (hemispheres)	
Bilateral	13
Right implant	2
Left implant	4
CRST score in the dominant hand (N = 12 hemispheres)	
Pre-CRST score in the dominant hand (mean ± SD)	12.2 ± 7.4
Post-CRST score in the dominant hand (mean ± SD)	4.0 ± 3.0
CRST score in the nondominant hand (N = 9)	
Pre-CRST score in the nondominant hand (mean ± SD)	10.7 ± 5.8
Post-CRST score in the nondominant hand (mean ± SD)	4.0 ± 3.8

CRST, Clinical Rating Scale for Tremor; DBS, deep brain stimulation; SD, standard deviation.

The empirically chosen active contacts (6.5 ± 1.7 months after surgery) were above the bicommissural plane in all hemispheres (4.95 ± 1.81 mm; Methods and Table, **Supplemental Digital Content**, http://links.lww.com/NEU/B50). The 3-dimensional Euclidean distance from the active contact to the probDRTT was 3.32 ± 1.70 mm, which was smaller than the distance to the detDRTT (5.01 ± 2.12 mm; $P < 10^{-4}$).

DISCUSSION

We compared the locations of the DRTT reconstructed with probabilistic vs deterministic tracking in the context of tremor surgery. In 19 patients with ET who underwent DBS implant (34 hemispheres) with intraoperative neurophysiology and stimulation testing, we used as a comparison reference the location of the active contacts, chosen based on clinical response by subspecialist neurologists. Our main finding was that the probDRTT (3.32 ± 1.70 mm) was closer to the active contact compared with the detDRTT (5.01 ± 2.12 mm). Notably, the distance from the

TABLE 2. DBS Lead and DRTT Coordinates in the Bicommissural Plane

	Lateral distance from AC–PC line (mm)	Anterior distance from PC (mm)
DBS leads	12.05 ± 1.35	5.19 ± 0.91
ProbDRTT	11.76 ± 2.04	6.64 ± 1.64
DetDRTT	14.22 ± 2.27	6.85 ± 2.21

AP–PC, anterior commissure–posterior commissure; DBS, deep brain stimulation; DRTT, dentato-rubro-thalamic tract; PC, posterior commissure; SD, standard deviation.

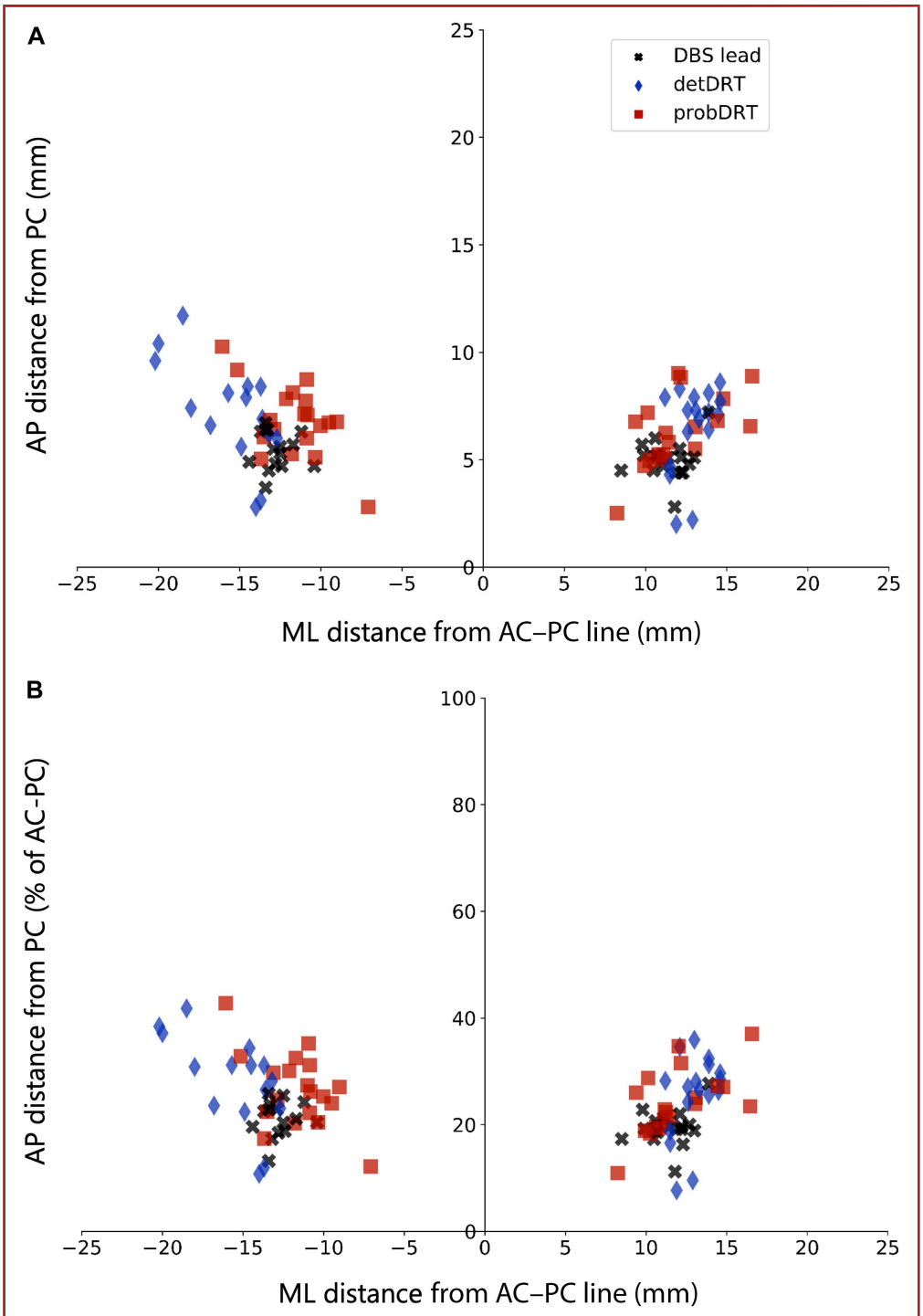

FIGURE 3. *Coordinates of the centroids of DBS leads, detDRTT, and probDRTT in the bicommissural plane.* **A**, *AP coordinates as absolute distance (mm) from the PC.* **B**, *AP coordinates as percentage of AC-PC length. AP, anteroposterior; AC, anterior commissure; DBS, deep brain stimulation; detDRTT, deterministic dentato-rubro-thalamic tract; PC, posterior commissure; probDRTT, probabilistic tractography deterministic dentato-rubro-thalamic tract.*

active contact to the probDRTT is congruent with the radius of stimulation spread (≈2.5-4 mm) based on computational modeling and experimental data.[32-34] To the best of our knowledge, this is the first study to provide evidence that probabilistic tractography results in superior reconstruction of the DRTT when compared with deterministic tractography.

From a practical standpoint, deterministic tractography offers distinct advantages over probabilistic techniques, which include integration into commercially available, Food and Drug Administration-approved surgical targeting software, ease of implementation, and reduced computational load (on the order of minutes vs hours). However, the DRTT is a complex cerebellothalamic tract with decussating and nondecussating pathways, and deterministic tractography is limited for resolving complex intravoxel fiber arrangements. Our data, along with the limited number of previous comparative studies,[13,14] demonstrate that deterministic methods are successful in reconstructing the DRTT only in a minority of cases (17%-62%) vs in 100% of cases with probabilistic techniques.

A growing body of literature has provided clinical validation of the DRTT visualized with either deterministic or probabilistic methods.[35] Building on these studies, our data suggest that direct targeting of the probDRTT may yield a greater clinical benefit vs targeting the detDRTT. However, tractography-based targeting engenders ambiguity in terms of where along the tract in three-dimensional space the optimal target may be. Established targeting methods (ie, atlas-based formulas) offer a straightforward approach by constraining targets to within the bicommissural plane. Hence, DBS leads are implanted with an anterolateral to posteromedial angle of approach, whereby the available contacts span the craniocaudal extent of the VIM above the bicommissural plane. We speculate that simply targeting the probDRTT in the bicommissural plane may be oversimplistic. Future studies should investigate placement of leads that takes into account the complex 3-dimensional course of the DRTT, eg, as it traverses horizontally from the VIM toward the motor cortex (as shown in Figure 2).

Limitations

There are some limitations to our study. Although we observed that the distance from active contact to probDRTT was smaller than the distance to detDRTT, a correlation with the degree of tremor reduction (eg, with the CRST) was prohibited because these data were only available in a subset of patients. Moreover, we emphasize that because DBS leads were implanted in most hemispheres after physiological mapping along a single tract, it is impossible to ascertain whether the empirically chosen location of the active contact represents the globally optimal target (ie, sampling error). However, such a granular physiological mapping during DBS surgery is fundamentally limited, given the constraints of current state-of-the-art surgical approaches and ethical concerns in patient care.

CONCLUSION

The probabilistic DRTT was spatially more congruent with the location of physiology-guided DBS leads and the location of the clinically optimal active contacts, providing both physiological and clinical support that probabilistic tracking leads to superior reconstruction of the DRTT when compared with deterministic tracking.

Funding

This research was supported by National Institutes of Health (NIH) grant R01NS096606 (PI: Dr Verma).

Disclosures

The authors have no personal, financial, or institutional interest in any of the drugs, materials, or devices described in this article.

REFERENCES

1. Benabid AL, Pollak P, Hoffmann D, et al. Long-term suppression of tremor by chronic stimulation of the ventral intermediate thalamic nucleus. *Lancet.* 1991; 337(8738):403-406.
2. Morel A, Magnin M, Jeanmonod D. Multiarchitectonic and stereotactic atlas of the human thalamus. *J Comp Neurol.* 1997;387(4):588-630.
3. Spiegelmann R, Nissim O, Daniels D, Ocherashvilli A, Mardor Y. Stereotactic targeting of the ventrointermediate nucleus of the thalamus by direct visualization with high-field MRI. *Stereotact Funct Neurosurg.* 2006;84(1):19-23.
4. Forstmann BU, Isaacs BR, Temel Y. Ultra high field MRI-guided deep brain stimulation. *Trends Biotechnol.* 2017;35(10):904-907.
5. Papavassiliou E, Rau G, Heath S, et al. Thalamic deep brain stimulation for essential tremor: relation of lead location to outcome. *Neurosurgery.* 2004;54(5): 1120-1129; discussion 1129-1130.
6. Rouiller EM, Liang F, Babalian A, Moret V, Wiesendanger M. Cerebellothalamocortical and pallidothalamocortical projections to the primary and supplementary motor cortical areas: a multiple tracing study in macaque monkeys. *J Comp Neurol.* 1994;345(2):185-213.
7. Asanuma C, Thach WR, Jones EG. Anatomical evidence for segregated focal groupings of efferent cells and their terminal ramifications in the cerebellothalamic pathway of the monkey. *Brain Res.* 1983;286(3):267-297.
8. Gallay MN, Jeanmonod D, Liu J, Morel A. Human pallidothalamic and cerebellothalamic tracts: anatomical basis for functional stereotactic neurosurgery. *Brain Struct Funct.* 2008;212(6):443-463.
9. Mollink J, van Baarsen KM, Dederen PJWC, et al. Dentatorubrothalamic tract localization with postmortem MR diffusion tractography compared to histological 3D reconstruction. *Brain Struct Funct.* 2016;221(7):3487-3501.
10. Calabrese E, Hickey P, Hulette C, et al. Postmortem diffusion MRI of the human brainstem and thalamus for deep brain stimulator electrode localization. *Hum Brain Mapp.* 2015;36(8):3167-3178.
11. Meola A, Comert A, Yeh F-C, Sivakanthan S, Fernandez-Miranda JC. The nondecussating pathway of the dentatorubrothalamic tract in humans: human connectome-based tractographic study and microdissection validation. *J Neurosurg.* 2016;124(5):1406-1412.
12. Nowacki A, Schlaier J, Debove I, Pollo C. Validation of diffusion tensor imaging tractography to visualize the dentatorubrothalamic tract for surgical planning. *J Neurosurg.* 2018;130(1):99-108.
13. Sammartino F, Krishna V, King NKK, et al. Tractography-based ventral intermediate nucleus targeting: novel methodology and intraoperative validation. *Mov Disord.* 2016;31(8):1217-1225.
14. Schlaier JR, Beer AL, Faltermeier R, et al. Probabilistic vs. deterministic fiber tracking and the influence of different seed regions to delineate cerebellar-thalamic fibers in deep brain stimulation. *Eur J Neurosci.* 2017;45(12):1623-1633.
15. Calamante F. The seven deadly sins of measuring brain structural connectivity using diffusion MRI streamlines fibre-tracking. *Diagnostics (Basel).* 2019;9(3):E115.

16. Jbabdi S, Johansen-Berg H. Tractography: where do we go from here? *Brain Connect.* 2011;1(3):169-183.
17. Chazen JL, Sarva H, Stieg PE, et al. Clinical improvement associated with targeted interruption of the cerebellothalamic tract following MR-guided focused ultrasound for essential tremor. *J Neurosurg.* 2018;129(2):315-323.
18. King NKK, Krishna V, Basha D, et al. Microelectrode recording findings within the tractography-defined ventral intermediate nucleus. *J Neurosurg.* 2017;126(5):1669-1675.
19. Yang AI, Buch VP, Heman-Ackah SM, et al. Thalamic deep brain stimulation for essential tremor: relation of the dentatorubrothalamic tract with stimulation parameters. *World Neurosurg.* 2020;137:e89-e97.
20. Kramer DR, Halpern CH, Buonacore DL, et al. Best surgical practices: a stepwise approach to the University of Pennsylvania deep brain stimulation protocol. *Neurosurg Focus.* 2010;29(2):E3.
21. Manjón JV, Coupé P, Concha L, Buades A, Collins DL, Robles M. Diffusion weighted image denoising using overcomplete local PCA. *PLoS One.* 2013;8(9):e73021.
22. Andersson JLR, Sotiropoulos SN. An integrated approach to correction for off-resonance effects and subject movement in diffusion MR imaging. *Neuroimage.* 2016;125:1063-1078.
23. Smith SM, Jenkinson M, Woolrich MW, et al. Advances in functional and structural MR image analysis and implementation as FSL. *Neuroimage.* 2004; 23(suppl 1):S208-S219.
24. Avants BB, Tustison NJ, Song G, Cook PA, Klein A, Gee JC. A reproducible evaluation of ANTs similarity metric performance in brain image registration. *Neuroimage.* 2011;54(3):2033-2044.
25. Doshi J, Erus G, Ou Y, et al. MUSE: MUlti-atlas region segmentation utilizing ensembles of registration algorithms and parameters, and locally optimal atlas selection. *Neuroimage.* 2016;127:186-195.
26. Tournier J-D, Calamante F, Connelly A. MRtrix: diffusion tractography in crossing fiber regions. *Int J Imaging Syst Technol.* 2012;22(1):53-66.
27. Tournier J-D, Calamante F, Connelly A. Improved probabilistic streamlines tractography by 2nd order integration over fibre orientation distributions. In: Proceedings of the international society for magnetic resonance in medicine; 2010.
28. Fischl B, van der Kouwe A, Destrieux C, et al. Automatically parcellating the human cerebral cortex. *Cereb Cortex.* 2004;14(1):11-22.
29. Elias WJ, Lipsman N, Ondo WG, et al. A randomized trial of focused ultrasound thalamotomy for essential tremor. *New Engl J Med.* 2016;375(8):730-739.
30. Yushkevich PA, Piven J, Hazlett HC, et al. User-guided 3D active contour segmentation of anatomical structures: significantly improved efficiency and reliability. *Neuroimage.* 2006;31(3):1116-1128.
31. Dhollander T, Emsell L, Van Hecke W, Maes F, Sunaert S, Suetens P. Track orientation density imaging (TODI) and track orientation distribution (TOD) based tractography. *Neuroimage.* 2014;94:312-336.
32. Mädler B, Coenen VA. Explaining clinical effects of deep brain stimulation through simplified target-specific modeling of the volume of activated tissue. *AJNR Am J Neuroradiol.* 2012;33(6):1072-1080.
33. Butson CR, Maks CB, McIntyre CC. Sources and effects of electrode impedance during deep brain stimulation. *Clin Neurophysiol.* 2006;117(2):447-454.
34. Miocinovic S, Lempka SF, Russo GS, et al. Experimental and theoretical characterization of the voltage distribution generated by deep brain stimulation. *Exp Neurol.* 2009; 216(1):166-176.
35. Gravbrot N, Saranathan M, Pouratian N, Kasoff WS. Advanced imaging and direct targeting of the motor thalamus and dentato-rubro-thalamic tract for tremor: a systematic Review. *Stereotact Funct Neurosurg.* 2020;98(4):220-240.

CNS Journal Club Podcast *and CME Exams available at cns.org/podcasts.*

Supplemental digital content *is available for this article at neurosurgery-online.com.*

Supplemental Digital Content. Methods and Table. Supplemental methods on active contact centroid calculation and active contact information.